Multi-objective H_2/H_∞/impulse-to-peak control of a space launch vehicle

D. Arzelier[1] B. Clement[2] D. Peaucelle[1]

1- LAAS-CNRS, 7 Avenue du Colonel Roche, 31 077 Toulouse, Cedex 4, France
emails: arzelier@laas.fr, peaucell@laas.fr
2- CNES Launcher directorate, Rond Point de l'Espace 91003 Evry Cedex, France
email: benoit.clement@cnes.fr

Abstract

A multi-objective synthesis problem involving H_2, H_∞ and impulse-to-peak performances is investigated. In general, multi-objective control problems are hard problems to solve and do not have exact solutions. Here, an LMI formulation is proposed for the mixed H_2/impulse-to-peak optimization under an H_∞ constraint for LTI discrete-time systems. This framework is then used to control the attitude of a space launcher. A particular control structure is defined and a multi-objective H_2/H_∞/impulse-to-peak synthesis problem is solved to tackle specific specifications. A systematic synthesis procedure including the tuning of design parameters is defined and results from simulations are presented..

Keywords: Multi-objective Control, LMI Optimization, Launch Vehicles, Attitude Control, Robust Synthesis

1 Introduction

It is well-known that H_∞ synthesis guarantees robust stability in the face of worst-case disturbances while H_2 synthesis is more adapted to deal with nominal performance. When imposing transient specifications (overshoot, settling time) a less known approach is to guarantee a bound on the peak impulse response [3], [15], [18], [19]. Applications involving sharp and various specifications naturally result in considering a mixed design framework that can integrate optimal transient performance and robustness in a single controller. In particular, the last developments of space launchers in terms of structure (optimized composite) and versatile payloads make it necessary to take hard design constraints into account in the pilot design phase. In such an application, the controller should counter the effects of uncertainties and dispersions affecting the launcher parameters as well as the disturbances (winds shear and gusts) while ensuring a high level of reliable performance (low level of consumption). Here, the reliability means that the angle of attack and the angle of deflection of the actuator (thrust) should stay below a pre-specified level during all the atmospheric flight of the launcher. During the last ten years, some attempts have been made to tackle the complex problem of robust attitude control of a space launch vehicle via modern control synthesis methods [9], [4], [10]. Those efforts lead to the definition of the working group PIROLA (PIlotage RObuste des LAnceurs).

1.1 The working group PIROLA

PIROLA was a three years research working group on robust control of launchers. This group, with financial support of CNES (French Space Agency) is aimed at improving control loop robustness and at reducing the time for tuning the control laws for this type of application. More specifically, the designer wishes to enlarge the controllable configurations and to allow the use of low cost sensors and actuators. The reduction of the time spent in tuning the control law

is obtained via the development of automatic procedures while keeping connection with physics. The group includes academic research partners: LAAS-CNRS (government research center) [1], [2], [17], ONERA (French aerospace research center) [20], [8], Supaero, [21], [22], Supelec [4], [5] (engineering schools) and an industrial partner: EADS ST (Space Transportation) [10].

Robust synthesis as well as robust analysis methodologies have been proposed in the frame of PIROLA. The former ranged from stationary control methodologies (H_∞ design based on the cross standard form, μ-synthesis, multi-objective control) to linear parameter-varying techniques and multi-model modal self-scheduled control while the last have mainly included techniques based on μ tools and SemiDefinite Programming (SDP) tools. The interested reader may consult the reference [8] for a more detailed information concerning the design methods. The goal of this article is to detail the LMI-based multi-objective control strategy proposed by LAAS-CNRS.

1.2 A multi-objective controller for launch vehicle control

Our approach consists in translating engineering requirements into automatic control specifications. These last specifications are converted into a particular multi-objective control problem involving H_2, H_∞ and impulse-to-peak performance criteria. As it turns out, despite the great number of papers on the subject, multi-objective synthesis problems are in general open problems except for some particular cases for which an exact convex formulation is given using LMI formalism. In our case, the best we can hope is to find a relaxed convex formulation as tight as possible since no exact convex characterization for the impulse-to-peak performance exists in the literature [18], [15], [19]. Here, a new characterization of impulse-to-peak performance is given for LTI discrete-time systems. It involves additional variables and allows a decoupling between the Lyapunov function and the system matrix in the spirit of references [7], [11], [14]. This property is particularly useful in robust and multi-objective control problems. Indeed, it paved the way for the reduction of inherent conservatism of robust or multi-objective control methods based on the Lyapunov shaping paradigm [15], [13], [12], [14], [1]. Here, an LMI formulation based on those ideas is proposed for the mixed H_2/impulse-to-peak optimization under an H_∞ constraint for LTI discrete-time systems. The relevance of the approach is illustrated by its application to the robust control of the attitude of a launch vehicle. An associated systematic synthesis procedure including the tuning of design parameters is defined and results from simulations are presented. These simulations are based on a very complete model including bending modes effects as well as time-varying behavior and non linear (rate and position limitations of actuators) effects. Future directions of research are then proposed in the concluding section.

1.3 Notations

Notation is standard. The transpose of a matrix A is denoted A'. For symmetric matrices, $>$ ($\geq$) denotes the Löwner partial order, i.e. $A > (\geq)\ B$ iff $A - B$ is positive (semi) definite. $\mathbf{1}$ stands for the identity matrix and $\mathbf{0}$ for the zero matrix with the appropriate dimensions. The symmetric part of a square matrix A is denoted $\mathrm{sym}[A]$, i.e. $\mathrm{sym}[A] = A + A'$.

2 Problem formulation

2.1 Ariane control loop

We are interested in the control of the launch vehicle during its atmospheric flight and particularly in the design of the piloting inner loop for the yaw axis of the launcher as illustrated by figure 1.

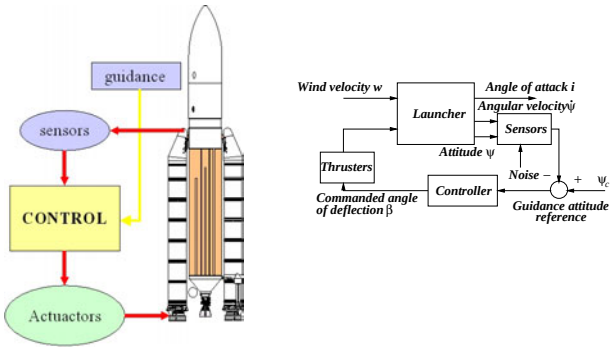

Figure 1: ARIANE control loop

The main function of this loop is to hold the launcher around its center of gravity which follows the guidance reference trajectory.

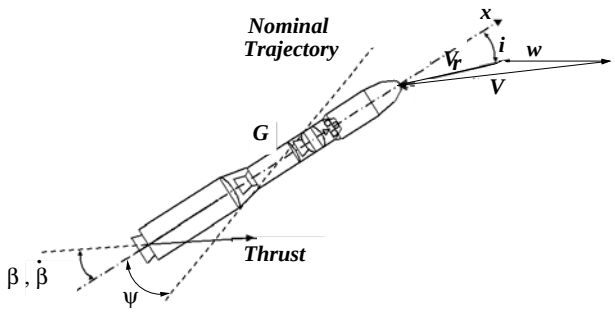

Figure 2: Model of the launcher

G is the center of gravity, V and V_r are the absolute and relative velocity and w is the wind velocity. i is the angle of attack and Ψ is the deviation of the launcher from the yaw axis with respect to the guidance attitude reference. The control variable is the thruster angle of deflection β. A thorough description of the plant may be found in the references [9], [4], [5].

2.2 Model of the launcher

To get a tractable analytical model for the plant, some simplifying assumptions have to be done.

Assumptions 1

- Axis are decoupled
- All angles remain small
- Parameters are slowly time-varying

Under these assumptions, the linearized dynamics of the launcher include a rigid model (without bending modes and actuator dynamics) where $\dot{\psi}$ is the angular velocity and $\dot{z}$ the lateral drift rate.

$$\begin{aligned} \ddot{\psi}(t) &= A_6 \left(\psi(t) + \frac{\dot{z}(t) - w(t)}{V} \right) + K_1 \beta(t) \\ \ddot{z}(t) &= a_1 \psi(t) + a_2 \left(\dot{z}(t) - w(t) \right) + a_3 \beta(t) \end{aligned} \tag{1}$$

Moreover, the angle of attack equation reads:

$$i(t) = \psi(t) + \frac{\dot{z}(t) - w(t)}{V} \tag{2}$$

Those equations depend on known aerodynamic coefficients $a_i,\ i = 1, 2, 3$ and time-varying coefficients A_6, the aerodynamic efficiency and K_1, the thruster efficiency along the flight envelope.

Defining the state vector as $x = \left[\ \Psi \quad \dot{\Psi} \quad \dot{z}\ \right]'$, the perturbation input as w and the controlled output as i, we get the following third-order state-space model for the rigid part of the launcher.

$$\begin{aligned} \dot{x}(t) &= \begin{bmatrix} 0 & 1 & 0 \\ A_6 & 0 & \frac{A_6}{V} \\ a_1 & 0 & a_2 \end{bmatrix} x(t) + \begin{bmatrix} 0 \\ -\frac{A_6}{V} \\ -a_2 \end{bmatrix} W + \begin{bmatrix} 0 \\ K_1 \\ a_3 \end{bmatrix} u(t) \\ z(t) = i(t) &= \begin{bmatrix} 1 & 0 & \frac{1}{V} \end{bmatrix} x(t) - \frac{1}{V} W \end{aligned} \tag{3}$$

Note that the launcher is aerodynamically unstable.

The sensors dynamics (second order for ψ and $\dot{\psi}$) and the actuators dynamics (second order) are added to the previous model to compose he complete linearized dynamics of the rigid launcher. Due to lack of tests and system complexity, internal uncertainties and dispersions have to be faced. They mainly concern the propulsion system, aerodynamic coefficients, mass model and inertia, flexible modes (elastic and sloshing), actuators and sensors modelling. The wind (shear and gusts) is considered as an external disturbance.

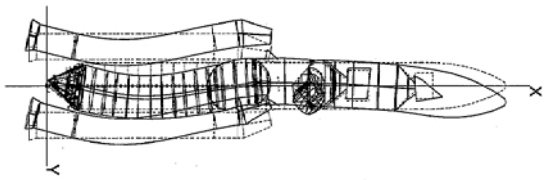

Figure 3: Bending modes of the ARIANE launcher

The first 5 bending modes are taken into account into the complete model and their characteristics are considered to be not exactly known (4 uncertain parameters per mode) leading to the definition of a discrete-time uncertain LFT simulation model of order 17 and $\Delta \in \mathbb{R}^{22\times 22}$.

2.3 Control objectives and performance specifications

During the atmospheric flight phase, the physical constraints and objectives defining the requirements that the pilot must fulfill are the following.

1- Guidance demand tracking.

2- Stabilize the launcher with respect to internal and external disturbances.

3- Limit the aerodynamical loads or equivalently limit angle of attack deviations.

4- Limit the consumption of the controller.

The physical constraints and objectives become automatic control requirements shaping the pilot.

- Closed-loop stability with sufficient stability margins (for a given flight time): Gain margins (low and high frequencies) must be respectively over LF and HF. Delay margin must be greater than one sampling period.

- In addition to the stability margins on the rigid part of the model, a specified attenuation of bending modes (X dB) has to be insured. The first flexible mode may be alternatively

controlled with respect to the previous defined attenuation X dB or with respect to its phase (see figure 4).

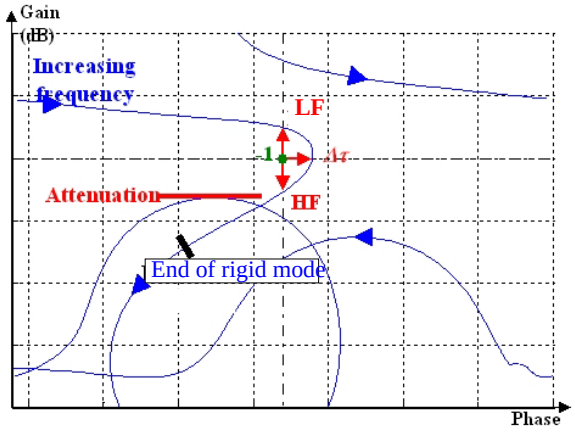

Figure 4: Illustration of the margins in the Nichols plot

- The pilot has to reject disturbances (wind and gusts) influence on the angle of attack i. In particular, angle of attack peaks must not exceed the limits $\pm\, i_{max}$ in response to a typical wind profile presented in figure 5.

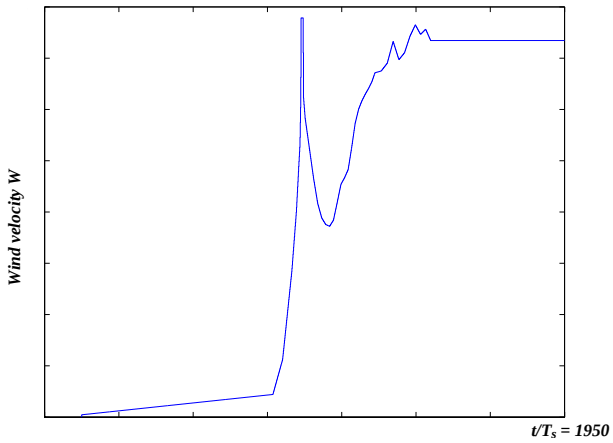

Figure 5: Wind profile

- The previous performance specifications must be achieved without an excessive thruster consumption expressed as cumulated deflections.

$$C = \sum_{k=T_{ini}}^{T_{end}} |\beta_{k+1} - \beta_k| \tag{4}$$

The pilot must make sure that robustness requirements with respect to uncertainties on the rigid and bending modes are fulfilled. This means that all previous control objectives have to be achieved for all possible configurations of the 22 uncertain parameters.

3 Multi-objective H_2/H_∞/impulse-to-peak design

Keeping in mind the high heterogeneity of the performance specifications, we adopt a multi-objective strategy for the control design procedure. Even if the problem of the synthesis of a

robust pilot achieving the different specifications may be naturally recast as a multi-objective control problem, it is first necessary to translate the control objectives and the performance specifications in terms of a set of design constraints involving adequate system norms. One therefore impose

- A bound on the impulse-to-peak performance of the closed-loop transfer $W - i$ with an additional filter modelling a typical wind profile to limit the angle of attack.
- A bound on the H_∞ performance of the sensitivity S to get a minimum modulus margin and therefore good gain margins
- A bound on the H_2 performance of the transfer between measurement noises and $\dot{\beta}$ to reduce the consumption
- A mixed roll-off and lead filter to attenuate the bending modes and control in phase the first one

The first step of the design procedure consists in choosing a particular model for synthesis purpose. Due to the high complexity of the complete model of the launcher, a simplified model is usually utilized for design purpose. Here, this simplified model is composed of the rigid model defined by the equation of the torque equilibrium of the yaw axis of the launcher. The synthesis model also includes the sensors dynamics (second order) but is free of the bending modes and actuator dynamics.

3.1 Structure of the controller

As will be seen in the next section, the controller is composed of two parts. One part of the controller is tuned (mixed filter) and the other part is computed via multi-objective optimization leading to the particular structure for the controller detailed in figure 6. Note also that the wind gust model acts like a weighting function which has to be tuned in the controller synthesis procedure.

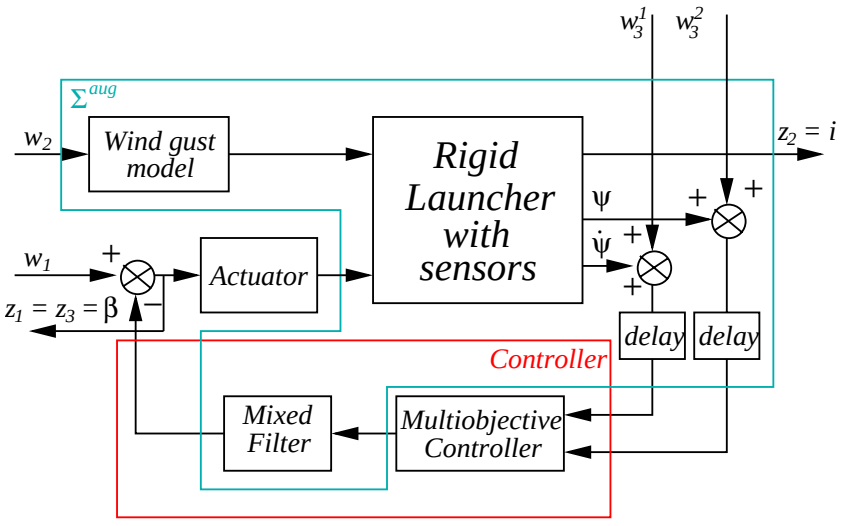

Figure 6: Structure of the multi-objective controller

The complete synthesis model is then defined by Σ^{aug}. An $H_2/H_\infty/\text{impulse} - \text{to} - \text{peak}$ multi-objective control problem is therefore set on Σ^{aug} to enforce the three first specifications.

3.2 The multi-objective control problem

3.2.1 Definition

Let the LTI discrete plant Σ^{aug} be given by its state-space minimal realization:

$$\begin{bmatrix} x_{k+1} \\ z_k \\ y_k \end{bmatrix} = \begin{bmatrix} A & B_1 & B \\ C_1 & D_{11} & D \\ C & D_{21} & \mathbf{0} \end{bmatrix} \begin{bmatrix} x_k \\ w_k \\ u_k \end{bmatrix} \tag{5}$$

where $x \in \mathbb{R}^n$ is the state vector, $w \in \mathbb{R}^{m_w}$ is the disturbance vector, $u \in \mathbb{R}^{m_u}$ is the input vector, $z \in \mathbb{R}^{r_z}$ is the controlled output vector and $y \in \mathbb{R}^{r_y}$ is the measured output vector.

The z and w vectors are partitioned as indicated in figure 7.

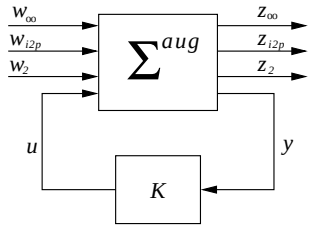

Figure 7: Standard model for multi-objective control

$$z = \begin{bmatrix} z_\infty \\ z_{i2p} \\ z_2 \end{bmatrix} \quad w = \begin{bmatrix} w_\infty \\ w_{i2p} \\ w_2 \end{bmatrix} \tag{6}$$

The associated matrices are therefore consequently partitioned.

$$\begin{gathered} B_1 = \begin{bmatrix} B_\infty & B_{i2p} & B_2 \end{bmatrix} \qquad C_1 = \begin{bmatrix} C_\infty \\ C_{i2p} \\ C_2 \end{bmatrix} \quad D_{11} = \begin{bmatrix} D_\infty & D_{\infty i2p} & D_{\infty 2} \\ D_{i2p\infty} & D_{i2p} & D_{i2p2} \\ D_{2\infty} & D_{2i2p} & D_2 \end{bmatrix} \\ D_{21} = \begin{bmatrix} D_{y\infty} & D_{yi2p} & D_{y2} \end{bmatrix} \quad D = \begin{bmatrix} D_{\infty u} \\ D_{i2pu} \\ D_{2u} \end{bmatrix} \end{gathered} \tag{7}$$

The controller K is given by its state-space realization:

$$\begin{aligned} \eta_{k+1} &= A_K \eta_k + B_K y_k \\ u_k &= C_K \eta_k + D_K y_k \end{aligned} \tag{8}$$

The closed-loop system $\Sigma^{aug.} \star K$ is given by its state-space matrices:

$$\begin{gathered} A_{cl} = \begin{bmatrix} A + BD_K C & BC_K \\ B_K C & A_K \end{bmatrix} \quad B_{cl} = \begin{bmatrix} B_1 + BD_K D_{21} \\ B_K D_{21} \end{bmatrix} \\ C_{cl} = \begin{bmatrix} C_1 + DD_K C & DC_K \end{bmatrix} \quad D_{cl} = [D_{11} + DD_K D_{21}] \end{gathered} \tag{9}$$

The multi-objective control problem is then defined in the following way.

PROBLEM 1 (**multi-objective $H_2/H_\infty/i2p$ control problem)**
Find a controller K in the set of internally stabilizing controllers $\mathcal{K}$ such that:

$$\begin{array}{ll} \min\limits_{K\in\mathcal{K}} & \alpha_i\gamma_{w-i} + \alpha_c\gamma_{cons} \\ \text{s.t.} & \\ & ||\Sigma_{mod}^{aug.} \star K||_\infty^2 \leq \gamma_{mod} \\ & ||\Sigma_{W-i}^{aug.} \star K||_{i2p}^2 \leq \gamma_{w-i} \\ & ||\Sigma_{cons}^{aug.} \star K||_2^2 \leq \gamma_{cons} \end{array} \tag{10}$$

If performance specifications are often expressed in terms of H_2 and H_∞ norms, impulse-to-peak performance is not so usual and deserve a thorough description.

3.2.2 The impulse-to-peak performance

At our knowledge, only references dealing with the continuous-time case may be found in the literature [3], [18], [15], [19].

Let the closed-loop discrete-time plant be given by its minimal realization:

$$\Sigma \star K \qquad \begin{array}{l} x_{k+1} = A_{cl}x_k + B_{cl}w_k \quad x(0) = 0 \\ z_k = C_{cl}x_k + D_{cl}w_k \end{array} \tag{11}$$

As in the continuous-time case, a conservative LMI characterization may be used to compute a bound on the peak of the impulse response of a discrete LTI system.

THEOREM 1
If there exists a matrix $\mathbf{P_{cl}} \in \mathbb{S}^{*+}$ and a scalar $\boldsymbol{\gamma^*}$ satisfying:

$$\begin{array}{rl} \gamma^* = \min\limits_{\mathbf{P_{cl}},\boldsymbol{\gamma}} & \boldsymbol{\gamma} \\ \text{s.t.} & \\ & A_{cl}\mathbf{P_{cl}}A_{cl}' - \mathbf{P_{cl}} < \mathbf{0} \\ & B_{cl}B_{cl}' - \mathbf{P_{cl}} < \mathbf{0} \\ & C_{cl}\mathbf{P_{cl}}C_{cl}' - \boldsymbol{\gamma}\mathbf{1} < \mathbf{0} \\ & D_{cl}D_{cl}' - \boldsymbol{\gamma}\mathbf{1} < \mathbf{0} \end{array} \tag{12}$$

then $||z_k||^2 \leq \gamma^* \ \ \forall\ k \geq 0$.

PROOF 1
First note that by Schur complement, all the inequalities defining the realizable set of (12 may be equivalently written with respect to $X_{cl} = P_{cl}^{-1}$:

$$A_{cl}'\mathbf{X_{cl}}A_{cl} - \mathbf{X_{cl}} < \mathbf{0} \tag{13}$$

$$B_{cl}'\mathbf{X_{cl}}B_{cl} < \mathbf{1} \tag{14}$$

$$\boldsymbol{\gamma}^{-\mathbf{1}}C_{cl}'C_{cl} - \mathbf{X_{cl}} < \mathbf{0} \tag{15}$$

$$\boldsymbol{\gamma}^{-\mathbf{1}}D_{cl}'D_{cl} - \mathbf{1} < \mathbf{0} \tag{16}$$

Let x and z be the solutions of (11) when the impulsive input w_{k_i} is applied with $x(0) = 0$. $w_{k_i} = \alpha e_i\delta_k,\ |\alpha| \leq 1,\ i = 1, \cdots, m_w$ where $e_i \in \mathbb{R}^{m_w}$ is the basis vector with 1 at the position i, 0 elsewhere and δ_k is the unit pulse. Then $\forall\ i$:

$$\begin{array}{ll} x_0 = 0 & z_0 = D_{cl}\alpha e_i \\ x_1 = B_{cl}\alpha e_i & z_1 = C_{cl}x_1 = C_{cl}B_{cl}\alpha e_i \\ x_k = A_{cl}^{k-1}B_{cl}\alpha e_i & z_k = C_{cl}x_k = C_{cl}A_{cl}^{k-1}B_{cl}\alpha e_i \end{array} \tag{17}$$

From (13), we get

$$x'_{k+1}X_{cl}x_{k+1} < x'_kX_{cl}x_k < \cdots < x'_1X_{cl}x_1$$

So, $\forall\ k \geq 1$, from (14) and (15),

$$1 > \alpha^2 B'_{cl}X_{cl}B_{cl} = x'_1X_{cl}x_1 > x'_kX_{cl}x_k > \gamma^{-1}x'_kC'_{cl}C_{cl}x_k \\ = \gamma^{-1}z'_kz_k$$

So, $||z_k||^2 < \gamma$. Using the last inequality (16) leads to

$$||z_0||^2 < \gamma\alpha^2 \leq \gamma$$

■

At our knowledge, this LMI characterization of the impulse-to-peak performance is new for discrete-time systems. Here, we are interested in an equivalent alternative LMI characterization of a bound on the impulse-to-peak performance of the closed-loop system (11). A generalization of the method in [13] where an extra matrix G is introduced for the test of H_2 and H_∞ performances leads to the equivalent LMI optimization problem.

THEOREM 2
Let the following semidefinite programming problem be given:

$$\begin{aligned} \gamma^*_G = \min_{\mathbf{P_{cl}},\boldsymbol{\gamma},\mathbf{G},\mathbf{F}} \quad & \boldsymbol{\gamma} \\ \text{s.t.} \quad & \begin{bmatrix} -\mathbf{P_{cl}} & A_{cl}\mathbf{G} \\ \mathbf{G}'A'_{cl} & \mathbf{P_{cl}} - \mathbf{G} - \mathbf{G}' \end{bmatrix} < \mathbf{0} \\ & \begin{bmatrix} -\mathbf{P_{cl}} & B_{cl} \\ B'_{cl} & -\mathbf{1} \end{bmatrix} < \mathbf{0} \\ & \begin{bmatrix} -\boldsymbol{\gamma}\mathbf{1} & C_{cl}\mathbf{F} \\ \mathbf{F}'C'_{cl} & \mathbf{P_{cl}} - \mathbf{F} - \mathbf{F}' \end{bmatrix} < \mathbf{0} \\ & \begin{bmatrix} -\boldsymbol{\gamma}\mathbf{1} & D_{cl} \\ D'_{cl} & -\mathbf{1} \end{bmatrix} < \mathbf{0} \end{aligned} \tag{18}$$

then

$$\gamma^* = \gamma^*_G$$

PROOF 2
The proof comes from the application of elimination lemma [16]) on the first and third inequality of (12). ■

So far, the new proposed characterization (18) of impulse-to-peak performance seems not to bring any novelty. In fact, we will see later that it allows to reduce the conservatism of the proposed bound when dealing with multi-objective control problem. The reference [1] gives another application of this condition in robust control context.

3.2.3 Impulse-to-peak performance design via LMI's

The previous characterization may be used to tackle the problem of designing a controller minimizing a bound on the impulse-to-peak performance.

PROBLEM 2 (**worst-case i2pk synthesis)**
Find a full-order dynamic output-feedback controller K in the set of internally stabilizing controllers $\mathcal{K}$.

$$\min_{K\in\mathcal{K}} ||\Sigma^{aug.} \star K||_{i2p} \quad = \quad \min_{K\in\mathcal{K}} \sup_{w\in I} ||z||_{\mathcal{L}_\infty} \tag{19}$$

where $I = \{w_{k_i} = \alpha e_i \delta_k,\ |\alpha| \leq 1,\ i = 1, \cdots, m_w\}$.

To address the impulse-to-peak performance synthesis problem, we need to relax the previous optimization problem (18) by setting $G = F$. This relaxation is known as the generalized shaping paradigm [13].

THEOREM 3
If there exist $\mathbf{X} \in \mathbb{R}^{n\times n}$, $\mathbf{Y} \in \mathbb{R}^{n\times n}$, $\hat{\mathbf{A}} \in \mathbb{R}^{n\times n}$, $\hat{\mathbf{B}} \in \mathbb{R}^{n\times r}$, $\hat{\mathbf{C}} \in \mathbb{R}^{m\times n}$, $\hat{\mathbf{D}} \in \mathbb{R}^{m\times r}$, $\mathbf{Q} \in \mathcal{S}_n^{+*}$, $\mathbf{H} \in \mathcal{S}_n^{+*}$, $\mathbf{J} \in \mathbb{R}^{n\times n}$, and a scalar $\boldsymbol{\gamma}_G^* \in \mathbb{R}^{+*}$ such that:

$$\begin{aligned}
\boldsymbol{\gamma}_G^* = \quad & \min_{\substack{\mathbf{X},\mathbf{Y},\boldsymbol{\gamma} \\ \mathbf{J},\mathbf{H},\mathbf{Q},\mathbf{S}}} \quad \boldsymbol{\gamma} \\
& s.t \\
& \begin{bmatrix} -\mathbf{Q} & -\mathbf{J} & A\mathbf{X}+B\hat{\mathbf{C}} & A+B\hat{\mathbf{D}}C \\ \star & -\mathbf{H} & \hat{\mathbf{A}} & \mathbf{Y}A+\hat{\mathbf{B}}C \\ \star & \star & \mathbf{Q}-\mathbf{X}-\mathbf{X}' & \mathbf{J}-\mathbf{S}'-\mathbf{1} \\ \star & \star & \star & \mathbf{H}-\mathbf{Y}-\mathbf{Y}' \end{bmatrix} < \mathbf{0} \\
& \begin{bmatrix} -\mathbf{Q} & -\mathbf{J} & B_{i2p}+B\hat{\mathbf{D}}D_{i2py} \\ \star & -\mathbf{H} & \mathbf{Y}B_{i2p}+\hat{\mathbf{B}}D_{i2py} \\ \star & \star & \mathbf{1} \end{bmatrix} < \mathbf{0} \\
& \begin{bmatrix} -\boldsymbol{\gamma} & C_{i2p}\mathbf{X}+D_{i2pu}\hat{\mathbf{C}} & C_{i2p}+D_{i2pu}\hat{\mathbf{D}}C \\ \star & \mathbf{Q}-\mathbf{X}-\mathbf{X}' & \mathbf{J}-\mathbf{S}'-\mathbf{1} \\ \star & \star & \mathbf{H}-\mathbf{Y}-\mathbf{Y}' \end{bmatrix} < \mathbf{0} \\
& \begin{bmatrix} -\boldsymbol{\gamma} & D_{i2p}+D_{i2pu}\hat{\mathbf{D}}D_{i2py} \\ \star & -\mathbf{1} \end{bmatrix} < \mathbf{0}
\end{aligned} \tag{20}$$

then a full-order controller reconstructed as follows:

$$\begin{aligned}
V_1'U_1 &= \mathbf{S}-\mathbf{Y}\mathbf{X} & D_K &= \hat{\mathbf{D}} \\
C_K &= (\hat{\mathbf{C}}-\hat{\mathbf{D}}C\mathbf{X})U_1^{-1} & B_K &= V_1^{-T}(\hat{\mathbf{B}}-\mathbf{Y}B\hat{\mathbf{D}}) \\
A_K &= V_1^{-T}\left[\hat{\mathbf{A}}-\mathbf{Y}(A+B\hat{\mathbf{D}}C)\mathbf{X}-V_1'B_KC\mathbf{X}-\mathbf{Y}BC_KU_1\right]U_1^{-1}
\end{aligned} \tag{21}$$

leads to bound the peak value of impulse response of the system:

$$||z||_\infty < \sqrt{\gamma_G^*}$$

PROOF 3
From (2), it is easy to see that the matrix G is invertible and may be partitioned as follows:

$$G = \begin{bmatrix} X & U_2 \\ U_1 & \bullet \end{bmatrix} \quad G^{-1} = \begin{bmatrix} Y & V_2 \\ V_1 & \bullet \end{bmatrix} \tag{22}$$

Then applying the following similarity transformation on the closed-loop Lyapunov matrix, we get:

$$\left[\begin{array}{cc} \mathbf{1} & \mathbf{0} \\ Y' & V_1' \end{array}\right] P_{cl} \left[\begin{array}{cc} \mathbf{1} & Y \\ \mathbf{0} & V_1 \end{array}\right] = \left[\begin{array}{cc} Q & J \\ J' & H \end{array}\right] \tag{23}$$

Multiplying the first three terms in (2) by $\left[\begin{array}{cc} \mathbf{1} & Y \\ \mathbf{0} & V_1 \end{array}\right]$ and by its transpose, we get the final result by applying the change of variables (21). ■

This parameterization is a slight modification of the one proposed in [15] and an extension to the impulse-to-peak case of the one given for the first time in the context of H_2 and H_∞ performances in [13]. Its main interest relies in the decoupling between the Lyapunov function and the computation of the controller. The controller is now built from the additional variable G allowing to use independent Lyapunov function in the context of multi-objective control.

3.3 LMI formulation of the multi-objective control problem

Let us come back to our original multi-objective control problem (10). Except in some particular cases, this problem is hard to solve analytically. Even if many sub-optimal numerical approaches have been developed, the reduction of the conservatism of the proposed solution is still a challenging problem, [18], [15]. In the previous subsection, we have seen how to convert the original worst-case impulse-to-peak design problem to a convex optimization problems involving LMIs. The same technique may be applied to the H_2 and H_∞ performance criteria as originally proposed in [13] and an extended LMI formulation may be formulated for H_∞ and H_2 performances of respectively $\Sigma_{mod.}^{aug.} \star K$ and $\Sigma_{cons.}^{aug.} \star K$.
H_∞ performance:

$$\left[\begin{array}{ccc} B_{\infty cl}B_{\infty cl}' - \mathbf{P_{\infty cl}} & B_{\infty cl}D_{\infty cl}' & \mathbf{0} \\ \star & -\boldsymbol{\gamma_{mod}}\mathbf{1} + D_{\infty cl}D_{\infty cl}' & \mathbf{0} \\ \star & \star & \mathbf{P_{\infty cl}} \end{array}\right] + \mathrm{sym}\left[\left[\begin{array}{c} A_{cl} \\ C_{\infty cl} \\ -\mathbf{1} \end{array}\right] \left[\begin{array}{ccc} \mathbf{0} & \mathbf{0} & \mathbf{G_\infty} \end{array}\right]\right] < \mathbf{0} \tag{24}$$

H_2 performance:

$$\begin{array}{l} \mathrm{trace}(\mathbf{T}) < \boldsymbol{\gamma_{cons}} \\ \\ \left[\begin{array}{ccc} -\mathbf{1} & B_{2cl}' & \mathbf{0} \\ B_{2cl} & -\mathbf{P_{2cl}} & \mathbf{0} \\ \star & \star & \mathbf{P_{2cl}} \end{array}\right] + \mathrm{sym}\left[\left[\begin{array}{c} \mathbf{0} \\ A_{cl} \\ -\mathbf{1} \end{array}\right] \left[\begin{array}{ccc} \mathbf{0} & \mathbf{0} & \mathbf{G_2} \end{array}\right]\right] < \mathbf{0} \\ \\ \left[\begin{array}{cc} -\mathbf{T} + D_{2cl}D_{2cl}' & \mathbf{0} \\ \star & \mathbf{P_{2cl}} \end{array}\right] + \mathrm{sym}\left[\left[\begin{array}{c} C_{2cl} \\ -\mathbf{1} \end{array}\right] \left[\begin{array}{cc} \mathbf{0} & \mathbf{G_2} \end{array}\right]\right] < \mathbf{0} \end{array} \tag{25}$$

Defining the notations

$$\begin{array}{rcl} \left[\begin{array}{cc} \mathbf{1} & \mathbf{0} \\ Y' & V_1' \end{array}\right] P_{2cl} \left[\begin{array}{cc} \mathbf{1} & Y \\ \mathbf{0} & V_1 \end{array}\right] & = & \left[\begin{array}{cc} Q_2 & J_2 \\ J_2' & H_2 \end{array}\right] \\ \\ \left[\begin{array}{cc} \mathbf{1} & \mathbf{0} \\ Y' & V_1' \end{array}\right] P_{\infty cl} \left[\begin{array}{cc} \mathbf{1} & Y \\ \mathbf{0} & V_1 \end{array}\right] & = & \left[\begin{array}{cc} Q_\infty & J_\infty \\ J_\infty' & H_\infty \end{array}\right] \\ \\ \left[\begin{array}{cc} \mathbf{1} & \mathbf{0} \\ Y' & V_1' \end{array}\right] P_{i2pcl} \left[\begin{array}{cc} \mathbf{1} & Y \\ \mathbf{0} & V_1 \end{array}\right] & = & \left[\begin{array}{cc} Q_{i2p} & J_{i2p} \\ J_{i2p}' & H_{i2p} \end{array}\right] \end{array} \tag{26}$$

a full-order output-feedback controller minimizing an upper bound for the multi-objective $H_2/H_\infty/i2p$ synthesis problem may be computed using semidefinite programming and LMI formulation.

THEOREM 4
If the following semidefinite programming problem has a solution

$$\begin{array}{c} \min \\ \mathbf{X},\mathbf{Y},\boldsymbol{\gamma_{cons}},\boldsymbol{\gamma_{w-i}},\mathbf{T},\mathbf{S} \\ \mathbf{J_i},\mathbf{H_i},\mathbf{Q_i},i=\infty,i2p,2 \end{array} \quad \alpha_c\boldsymbol{\gamma_{cons}}+\alpha_i\boldsymbol{\gamma_{w-i}}$$

under

$$\left[\begin{array}{cccccc} -\mathbf{Q}_\infty & -\mathbf{J}_\infty & A\mathbf{X}+B\hat{\mathbf{C}} & A+B\hat{\mathbf{D}}C & B_\infty+B\hat{\mathbf{D}}D_{y\infty} & \mathbf{0} \\ \star & -\mathbf{H}_\infty & \hat{\mathbf{A}} & \mathbf{Y}A+\hat{\mathbf{B}}C & \mathbf{Y}B_\infty+\hat{\mathbf{B}}D_{y\infty} & \mathbf{0} \\ \star & \star & \mathbf{Q}_\infty-\mathbf{X}-\mathbf{X}' & -\mathbf{1}-\mathbf{S}'+\mathbf{J}_\infty & \mathbf{0} & \mathbf{X}'C'_\infty+\hat{\mathbf{C}}'D'_{\infty u} \\ \star & \star & \star & \mathbf{H}_\infty-\mathbf{Y}-\mathbf{Y}' & \mathbf{0} & C'_\infty+C'\hat{\mathbf{D}}'D'_{\infty u} \\ \star & \star & \star & \star & -\mathbf{1} & D'_\infty+D'_{y\infty}\hat{\mathbf{D}}'D'_{\infty u} \\ \star & \star & \star & \star & \star & -\gamma_{mod}\mathbf{1} \end{array}\right]<\mathbf{0}$$

$$\left[\begin{array}{cccc} -\mathbf{Q_{i2p}} & -\mathbf{J_{i2p}} & A\mathbf{X}+B\hat{\mathbf{C}} & A+B\hat{\mathbf{D}}C \\ \star & -\mathbf{H_{i2p}} & \hat{\mathbf{A}} & \mathbf{Y}A+\hat{\mathbf{B}}C \\ \star & \star & \mathbf{Q_{i2p}}-\mathbf{X}-\mathbf{X}' & \mathbf{J_{i2p}}-\mathbf{S}'-\mathbf{1} \\ \star & \star & \star & \mathbf{H_{i2p}}-\mathbf{Y}-\mathbf{Y}' \end{array}\right]<\mathbf{0}$$

$$\left[\begin{array}{ccc} -\mathbf{Q_{i2p}} & -\mathbf{J_{i2p}} & B_{i2p}+B\hat{\mathbf{D}}D_{i2py} \\ \star & -\mathbf{H_{i2p}} & \mathbf{Y}B_{i2p}+\hat{\mathbf{B}}D_{i2py} \\ \star & \star & \mathbf{1} \end{array}\right]<\mathbf{0}$$

$$\left[\begin{array}{ccc} -\boldsymbol{\gamma_{w-i}} & C_{i2p}\mathbf{X}+D_{i2pu}\hat{\mathbf{C}} & C_{i2p}+D_{i2pu}\hat{\mathbf{D}}C \\ \star & \mathbf{Q_{i2p}}-\mathbf{X}-\mathbf{X}' & \mathbf{J_{i2p}}-\mathbf{S}'-\mathbf{1} \\ \star & \star & \mathbf{H_{i2p}}-\mathbf{Y}-\mathbf{Y}' \end{array}\right]<\mathbf{0}$$

$$\left[\begin{array}{cc} -\boldsymbol{\gamma_{w-i}} & D_{i2p}+D_{i2pu}\hat{\mathbf{D}}D_{i2py} \\ \star & -\mathbf{1} \end{array}\right]<\mathbf{0}$$

$\text{Trace}(\mathbf{T_2})<\boldsymbol{\gamma_{cons}}$

$$\left[\begin{array}{cccc} -\mathbf{T_2} & C_2\mathbf{X}+D_{2u}\hat{\mathbf{C}} & C_2+D_{2u}\hat{\mathbf{D}}C & D_2+D_{2u}\hat{\mathbf{D}}D_{y2} \\ \star & Q_2-\mathbf{X}-\mathbf{X}' & -\mathbf{1}-\mathbf{S}'+\mathbf{J_2} & \mathbf{0} \\ \star & \star & \mathbf{H_2}-\mathbf{Y}-\mathbf{Y}' & \mathbf{0} \\ \star & \star & \star & -\mathbf{1} \end{array}\right]<\mathbf{0}$$

$$\left[\begin{array}{ccccc} -\mathbf{Q_2} & -\mathbf{J_2} & A\mathbf{X}+B\hat{\mathbf{C}} & A+B\hat{\mathbf{D}}C & B_2+B\hat{\mathbf{D}}D_{y2} \\ \star & -\mathbf{H_2} & \hat{\mathbf{A}} & \mathbf{Y}A+\hat{\mathbf{B}}C & \mathbf{Y}B_2+\hat{\mathbf{B}}D_{y2} \\ \star & \star & \mathbf{Q_2}-\mathbf{X}-\mathbf{X}' & -\mathbf{1}-\mathbf{S}'+\mathbf{J_2} & \mathbf{0} \\ \star & \star & \star & \mathbf{H_2}-\mathbf{Y}-\mathbf{Y}' & \mathbf{0} \\ \star & \star & \star & \star & -\mathbf{1} \end{array}\right]<\mathbf{0}$$

(27)

then a controller K constructed from (21) is a suboptimal solution to the multi-objective synthesis problem (10).

PROOF 4
The proof is very simple and consists in creating a particular G_i matrix for each performance constraint. Applying a generalized shaping paradigm

$$G_\infty=G_{i2p}=G_2=G=\left[\begin{array}{cc} X & U_2 \\ U_1 & \bullet \end{array}\right] \quad G^{-1}=\left[\begin{array}{cc} Y & V_2 \\ V_1 & \bullet \end{array}\right] \tag{28}$$

and the linearizing change of variables

$$\begin{array}{l}\hat{D} = D_K \\ \hat{C} = C_K U_1 + \hat{D} C X \\ \hat{B} = V_1^{-1'} B_K + Y B \hat{D} \\ \hat{A} = V_1^{-1'} \hat{A} U_1 + Y(A + B\hat{B}C)X + V_1' B_K C X + Y B C_K U_1\end{array} \tag{29}$$

leads to the result. ■

Notice also that the proposed approach is always less conservative than the one using the Lyapunov Shaping paradigm from [15].

3.4 Synthesis procedure and tuning parameters

As seen before, the whole controller is formed from a mixed filter in series with a multi-objective controller. We have therefore two different sets of tuning parameters. The first set is formed with the parameters defining the wind gust model and the mixed filter. The wind gust model is a second order with two tuning parameters while the mixed filter is composed of a low-pass filter multiplied by a lead filter:

$$W_w(p) = \frac{K_w}{p^2 + 2T_w p + T_w^2} \quad W_m = \frac{1 + a\tau p}{1 + \tau p} \frac{K_{ro}}{1 + T_{ro} p} \tag{30}$$

We have therefore 6 synthesis parameters: K_W, T_W, K_{ro}, T_{ro}, a and τ. The other set of tuning parameters is formed from the optimization parameters α_i/α_c and γ_{mod} of the multi-objective LMI optimization step. The complete synthesis procedure therefore reads as

Algorithm 1

1- Choose the tuning parameters and form the augmented plant $\Sigma^{Aug.}$. Extract $\Sigma^{Aug.}_{w-i}$, $\Sigma^{Aug.}_{cons}$ and $\Sigma^{Aug.}_{mod}$.

2- Solve the convex optimization problem via LMI optimization and get the decision variables.

$$\begin{array}{ll}\min & (\alpha_i \gamma_{w-i} + \alpha_c\ \gamma_{cons}\ ) \\ \text{under} & \\ & \mathcal{L}_{\infty m}(\mathbf{Q}_m, \mathbf{J}_m, \mathbf{H}_m, \mathbf{X}, \mathbf{Y}, \mathbf{S}, \hat{\mathbf{A}}, \hat{\mathbf{B}}, \hat{\mathbf{C}}, \hat{\mathbf{D}}, \gamma_{mod}) < \mathbf{0} \\ & \mathcal{L}_{i2p}(\mathbf{Q}_{i2p}, \mathbf{J}_{i2p}, \mathbf{H}_{i2p}, \mathbf{X}, \mathbf{Y}, \mathbf{S}, \hat{\mathbf{A}}, \hat{\mathbf{B}}, \hat{\mathbf{C}}, \hat{\mathbf{D}}, \boldsymbol{\gamma_{w-i}}) < \mathbf{0} \\ & \mathcal{L}_{2c}(\mathbf{Q}_2, \mathbf{J}_2, \mathbf{H}_2, \mathbf{T}_2, \mathbf{X}, \mathbf{Y}, \mathbf{S}, \hat{\mathbf{A}}, \hat{\mathbf{B}}, \hat{\mathbf{C}}, \hat{\mathbf{D}}, \boldsymbol{\gamma_{cons}}) < \mathbf{0}\end{array} \tag{31}$$

3- Reconstruct the controller with formulae (21).

4 Simulation results

The previous algorithm has been used to design a robust autopilot for the atmospheric flight of a space launcher. Some worst-cases parametric configuration where the combination of parameter extremal values is particularly critical has been identified. The synthesis has been performed considering an LTI worst-case configuration of the time-varying parameters of the launcher. During the atmospheric flight phase, the time-variant behavior of the launcher and physical behavior is validated by simulations using a SIMULINK© model where information about specifications fulfillment is provided to the user. The time-domain specifications are therefore verified by inspecting the time responses provided by time-varying simulations while the frequency domain specifications are checked by considering only some pre-defined worst-cases. Indeed, the

robustness analysis of the frequency domain performances is limited to those worst-cases as the experience has shown that they are quite representative of the complete problem.

First, the Bode plot of the multi-objective controller computed via algorithm 1 is presented in figure 8. The effect of the lead filter is obvious for the channel $\psi - u$.

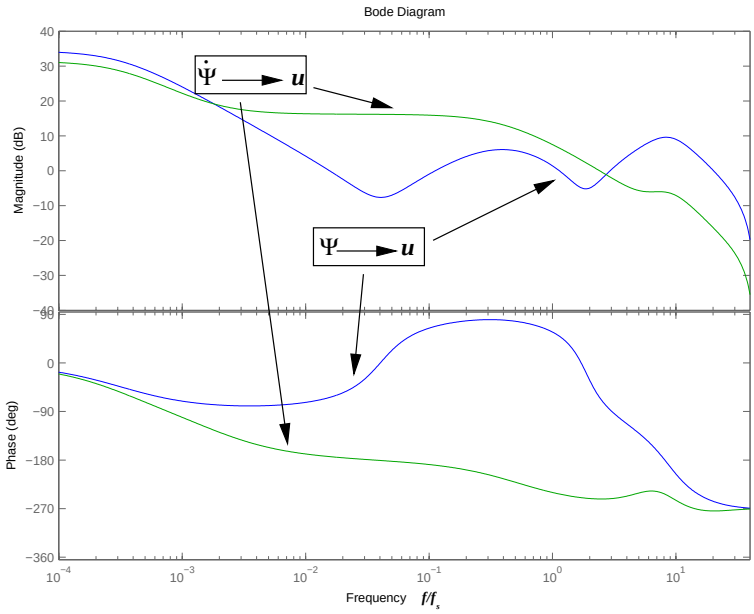

Figure 8: Bode diagram of the multi-objective pilot

The open-loop frequency responses are given in Nichols charts in figures 9 and 10 for several linearized models of specific configurations. This plot is obtained by freezing the model of the launcher when the wind gust is applied. The roll-off specification on bending modes is indicated by the $X\ dB$ horizontal line. A zoom on a specific range of frequencies allows to verify gain margins imposed on the rigid model. Note also that the first flexible mode remains between two critical points for all worst-cases satisfying the phase control requirement for this mode.

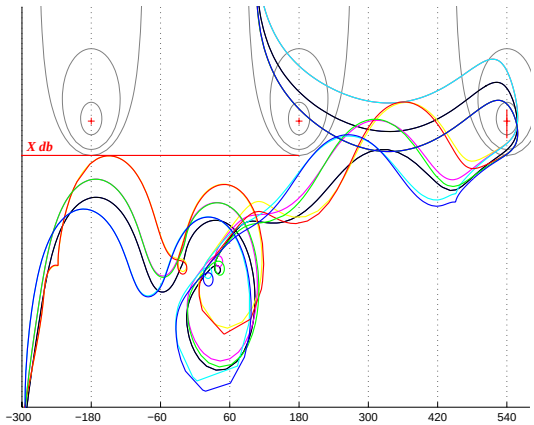

Figure 9: Nichols plot of the open-loop

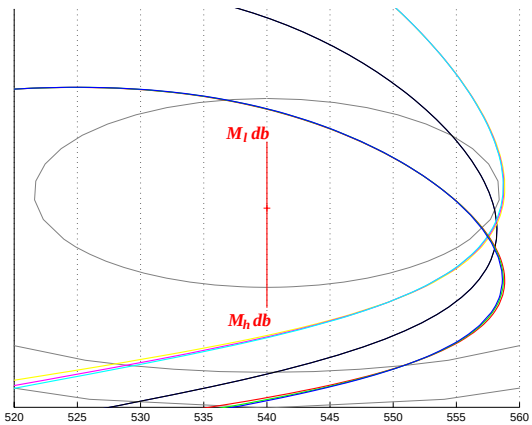

Figure 10: Zoom on the Nichols plot

Various time responses are also proposed. Note that all scales have been normalized with respect to the sample period T_s. The first figure shows the variation of the angle of attack when the typical wind profile in figure 5 is applied. The consumption $C = \sum_{k=T_{init}}^{T_{end}} |\beta(k+1) - \beta(k)|$ is computed and plotted with respect to the maximum allowed consumption. The right plot shows that the consumption is very good since the multi-objective controller needs only 50 % of the maximum allowable consumption to tackle the specifications.

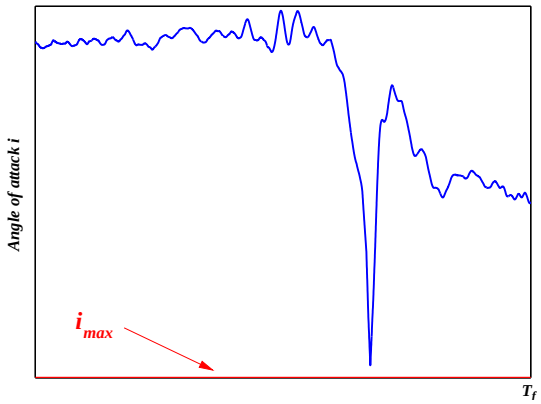

Figure 11: Angle of attack

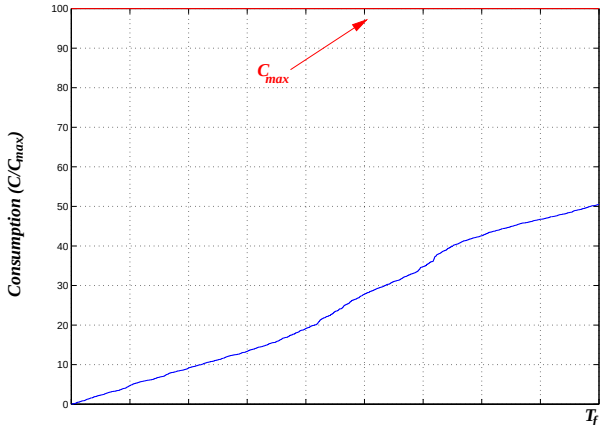

Figure 12: Consumption

Finally, the angle of deflection and its velocity are plotted below. They are far from the specified maxima.

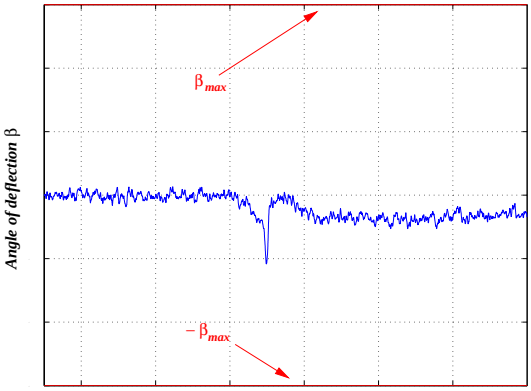

Figure 13: Angle of deflection

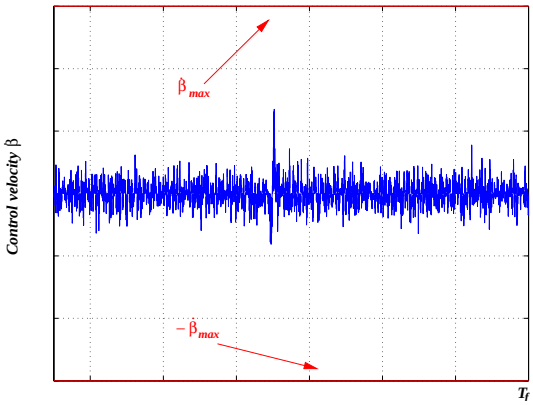

Figure 14: Velocity of the angle of deflection

5 Conclusions

The simulations have shown that this approach leads to controllers verifying all the specifications imposed on the launcher during the atmospheric flight. This black box-like method allows a great flexibility in the synthesis process. The tuning parameters are clearly identified with respect to the fundamental trade-off proposed by the performance specifications. Easy-to-use macros of MATLAB based on convex semidefinite optimization solvers allow the designer to tune adequately the synthesis parameters.

The main drawback of the proposed method comes from the fact that it can be used only with a simplified synthesis model (without bending modes) due to numerical considerations. Moreover, the parametric uncertainty of the model is not directly dealt with. In fact, parametric robustness concerns are inherited from time-varying nature of the model which is not taken into account here. Considering that the time spent to design a multi-objective controller is not prohibitive, the first step in order to take non stationarity into account would be to interpolate a finite number (5 or 6) of multi-objective controllers computed for a frozen configuration of the launcher all along the atmospheric flight envelope. Of course, this does not mean that finding an adequate interpolation algorithm is an easy task!

References

[1] D. Arzelier, D. Peaucelle, "Robust impulse-to-peak synthesis: Application to the control of an aerospace launcher", *Proceedings of the CCA/ISIC/CACSD*, Taipei, Taiwan, September 2004.

[2] D. Arzelier, D. Peaucelle, "Multiobjective H2/Hinfinity/impulse-to-peak synthesis: Application to the control of an aerospace launcher", *16th IFAC Symposium on Automatic Control in Aerospace, St Petersburg*, June 2004.

[3] S.P. Boyd, L.E. El Ghaoui, E. Feron, V. Balakrishnan, *Linear matrix inequalities in system and control theory*, SIAM Studies, 1994.

[4] B. Clement, G. Duc, "A multiobjective control algorithm: Application to a launcher with bending modes", *Proceedings of the 8th IEEE Mediterranean Conference on Control and Automation*, Rio Patras, Greece, 2000.

[5] B. Clement, G. Duc, S. Mauffrey, A. Biard, "Aerospace launch vehicle control: a gain scheduing approach", *15th triennial World Congress*, Barcelona, 2002.

[6] P. Gahinet, A. Nemirovski, A. Laub, M. Chilali, *LMI Control Toolbox*, LMI Control Toolbox User's Guide, 1995.

[7] J.C. Geromel, M.C. de Oliveira, L. Hsu, "LMI Characterization of structural and robust stability", *Linear Algebra and its Applications*, vol. 285, 1-3, pp. 69-80, December 1998.

[8] N. Imbert, B. Clement, "Launcher attitude control: some answers to the robustness issue", *16th IFAC Symposium on Automatic Control in Aerospace*, St Petersbourg, Russia, 2004.

[9] S. Mauffrey, M. Schoeller, "Non-stationnary H_∞ control for launcher with bending modes", *14th IFAC Symposium on Automatic Control in Aerospace*, Seoul, Korea, 1998.

[10] S. Mauffrey, P. Meunier, G. Pigni, A. Biard, I. Rongier, "H_∞ control for the ARIANE 5 plus Launcher", *52nd International Astraunotic Congress*, Toulouse, France, 2001.

[11] M.C. de Oliveira, J. Bernussou, J.C. Geromel, "A new discrete-time robust stability condition", *Systems & Control Letters*, Vol. 37, No. 4, July 1999.

[12] M.C. de Oliveira, J.C. Geromel, L. Hsu, "LMI Characterization of structural and robust stability: the discrete-time case", *Linear Algebra and its Applications*, Vol. 296, 1-3, pp.27-38, July 1999.

[13] M.C. Oliveira, J. Bernussou, J.C. Geromel, "Extended H_2 and H_∞ norm characterizations and controller parametrizations for discrete-time systems", *International Journal of Control*, Vol. 75, pp. 666-679, 2002.

[14] D. Peaucelle, D. Arzelier, O. Bachelier, J. Bernussou, "A new robust $\mathcal{D}$-stability condition for real convex polytopic uncertainty", *Systems & Control Letters*, vol. 40, 1, may 2000.

[15] C.W. Scherer, P. Gahinet, M. Chilali, "Multiobjective output-feedback control via LMI optimization", *IEEE Transactions on Automatic Control*, Vol. 42, No. 7, pp. 896-911, 1997.

[16] R.E. Skelton, T. Iwasaki, K. Grigoriadis, *A unified algebraic approach to linear control design*, Taylor and Francis, 1998.

[17] S.Tarbouriech , G.Garcia , P.Langouet, *Anti-windup strategy with guaranteed stability for linear systems with amplitude and dynamics restricted actuator*, 6th IFAC-Symposium on Nonlinear Control Systems (NOLCOS'2004), Stuttgart, Germany, pp.1373-1378, 1-3 September 2004.

[18] H. Tokunaga, T. Iwasaki, S. Hara, "Multi-objective robust control with transient specifications", *Proceedings of the 35th Conference on Decision and Control*, Kobe, Japan, 1996.

[19] H. Tokunaga, T. Iwasaki, S. Hara, "Analysis and synthesis of the robust impulse-to-peak performance", *Automatica*, Vol. 34, No. 11, pp. 1473-1477, 1998.

[20] O. Voinot, D. Alazard, A. Piquereau, "A robust multiobjective synthesis applied to launcher attitude control", *15th IFAC Symposium on Automatic Control in Aerospace*, Bologna, Italy, 2001.

[21] O. Voinot, P. Apkarian, D. Alazard, "Gain-Scheduling H_∞ control of the launcher in atmospheric flight via linear-parameter varying techniques", *AIAA Guidance, Navigation and —Control Conference*, Monterey, Ca, USA, August 2002.

[22] O. Voinot, D.Alazard, P. Apkarian, S. Mauffrey et B. Clment, "Launcher attitude control: discrete-time robust design and gain-scheduling", *Control Engineering Practice*, Vol. 11, Issue 11, November 2003.